



Magnetic resonance imaging-assessed synovial and bone changes in hand and wrist joints of rheumatoid arthritis patients

Kyung-Ann Lee¹, Sang-Ho Min², Tae-Hyung Kim³, Sang-Heon Lee¹, and Hae-Rim Kim¹

¹Division of Rheumatology, Department of Internal Medicine, Departments of ²Internal Medicine and ³Radiology, Konkuk University Medical Center, Seoul, Korea

Received: August 24, 2016
Revised : October 27, 2016
Accepted: February 22, 2017

Correspondence to
Hae-Rim Kim, M.D.

Division of Rheumatology,
Department of Internal Medicine,
Konkuk University Medical Center,
120-1 Neungdong-ro, Gwangjin-gu,
Seoul 05030, Korea
Tel: + 82-2-2030-7542
Fax: + 82-2-2030-7748
E-mail: kimhaerim@kuh.ac.kr

Background/Aims: Magnetic resonance imaging (MRI) is a sensitive and useful method for the detection of synovitis and joint destruction in rheumatoid arthritis (RA) patients. However, the patterns of MRI-detected bone erosion, bone marrow edema (BME), synovitis, and tenosynovitis have received insufficient attention. Therefore, this study evaluated the patterns of bone erosion, BME, synovitis, and tenosynovitis, and calculated the RA-MRI score (RAMRIS) of patients with RA at the carpal and metacarpophalangeal (MCP) joints using MRI.

Methods: MRI datasets from 43 RA patients were analyzed. All patients had undergone MRI of one wrist. In addition, 36 patients had MCP joint images taken, and three had also received MRI of the contralateral wrist and MCP joints. The MR images were evaluated for bone erosion, BME, and synovitis in consensus by two blinded readers according to the Outcome Measures in Rheumatology Clinical Trials (OMERACT) RAMRIS. The MRI-detected tenosynovitis was evaluated based on Haavardsholm's tenosynovitis score.

Results: The capitate, lunate, triquetrum, and hamate bones were the most common sites of erosion and BME and showed the highest RAMRIS erosion and BME scores. Moreover, MRI-detected tenosynovitis was present in 78.3% of all patients with RA, and the extensor compartment 4 and flexor digitorum profundus and superficialis were frequently affected.

Conclusions: This study identified the distribution and prevalence of MRI-detected bone erosion, BME, synovitis, and tenosynovitis of the wrist and MCP joints in RA patients. The patterns of the MRI-detected abnormalities may help to select sites for the application of MRI protocols in clinical trials and practice.

Keywords: Arthritis, rheumatoid; Magnetic resonance imaging; Synovitis; Tenosynovitis

INTRODUCTION

Rheumatoid arthritis (RA) is a systemic inflammatory disease that causes joint destruction through the erosion of cartilage and bone, and deformity through the stretching of tendons and ligaments [1,2]. Imaging mo-

dalities such as magnetic resonance imaging (MRI) and ultrasound have been developed for the detection of early RA and to impede destruction. MRI has demonstrated greater sensitivity than conventional radiography for the identification of early bone damage. Moreover, it also allows the detection of bone marrow edema,

synovitis, and tenosynovitis [3-6].

For a standardized and easily applicable MRI assessment system, the international Outcome Measures in Rheumatology Clinical Trials (OMERACT) MRI working group has developed a scoring system, the OMERACT RA-MRI score (RAMRIS), which includes semi-quantitative scores for bone erosion, bone marrow edema (BME), and synovitis of the wrist and metacarpophalangeal (MCP) joints [7-9]. In addition to the RAMRIS, a novel scoring system has been developed for tenosynovitis assessment [10]. In recent years, MRI has been used as a tool to measure the structural joint damage, disease activity, and response to treatment in RA clinical trials [11-15]. However, there has been little data on the distribution patterns of bone erosion, BME, synovitis, and tenosynovitis [16,17].

This study was designed to evaluate the prevalence of MRI-detected bone erosion, BME, synovitis, and tenosynovitis, and to investigate the RAMRIS at the wrist and MCP joints of RA patients. It then assesses the differences in the involved MRI patterns and the RAMRIS between patients with seropositive rheumatoid arthritis (SPRA) and those with seronegative rheumatoid arthritis (SNRA).

METHODS

Study design and study population

Patients with RA who had undergone MRI of the wrist or hand joints were selected for inclusion in this study through a retrospective review of medical records. All patients fulfilled the 2010 American College of Rheumatoid Arthritis classification criteria [18]. A total of 43 patients were enrolled. All patients had received MRI of one wrist. In addition, 36 patients had MCP joint MR images taken, and three patients had received additional MRI of the contralateral wrist and MCP joints. Basic demographic information was obtained for all patients, including their age, gender, disease duration, and treatment prior to the MRI scan. The patients' laboratory parameters at the time of the MRI scan, including their immunoglobulin M (IgM) rheumatoid factor (RF), anti-cyclic citrullinated peptides antibody (anti-CCP Ab), erythrocyte sedimentation rate (ESR), and C-reactive protein (CRP) levels, were also collected. This study was

approved by the Institutional Review Board for Human Research, Konkuk University Medical Center (KUH 1010815). The informed consent was waived under the IRB authority.

MRI scanning and scoring

The first-through-to-fifth MCP joints and the wrist of the most painful side—or of the dominant side in cases of equally severe symptoms on both sides—were scanned. The MRI was performed using a 3.0T Impact MRI unit (Skyra, Siemens, Erlangen, Germany) with a dual phased array wrist coil. All the MRI examinations (of the wrists and MCP joints) were carried out with T1-weighted echo and T2-weighted fat suppression sequences without intravenous contrast. The T1 coronal scanning measures were as follows: (1) repetition time (TR) = 600 msec, echo time (TE) = 10 msec, flip angle = 137°; (2) number of excitations (NEX) = 1; (3) field of view (FOV) = 192 × 220 mm; (4) matrix = 450 frequency, 310 phase; and (5) slice thickness = 2 mm, interslice gap = 2 mm. The T2 coronal scanning measures with fat suppression were as follows: (1) TR = 3,010 msec, TE = 55 msec, flip angle = 145°; (2) NEX = 1; (3) FOV = 220 × 220 mm; (4) matrix = 448 frequency, 358 phase; and (5) slice thickness = 2 mm, interslice gap = 2 mm. The T1 axial scanning measures were as follows: (1) TR = 640 msec, TE = 13 msec, flip angle = 134°; (2) NEX = 1; (3) FOV = 121 × 130 mm; (4) matrix = 510 frequency, 380 phase; and (5) slice thickness = 4 mm, interslice gap = 6 mm. The T2 axial scanning measures were as follows: (1) TR = 3,700 msec, TE = 56 msec, flip angle = 150°; (2) NEX = 1; (3) FOV = 121 × 129 mm; (4) matrix = 380 frequency, 250 phase; and (5) slice thickness = 4 mm, interslice gap = 6 mm.

The MR images were evaluated for bone erosion, bone edema, synovitis, and tenosynovitis in consensus by one board certified radiologist and one experienced rheumatologist who were blinded to other clinical information.

The MRI was assessed for the presence/absence and the semiquantitative scores of bone erosion, bone marrow edema, and synovitis according to the OMERACT RAMRIS without contrast injection (Fig. 1A and 1B). The sites included for scoring based on the hand MR images were: the first-through-to-fifth MCP joints, the carpal bones, the distal radius, the distal ulnar, and the radiocarpal, intercarpal, carpometacarpal (CMC), and distal radio-ulnar joints. MRI-detected bone erosion

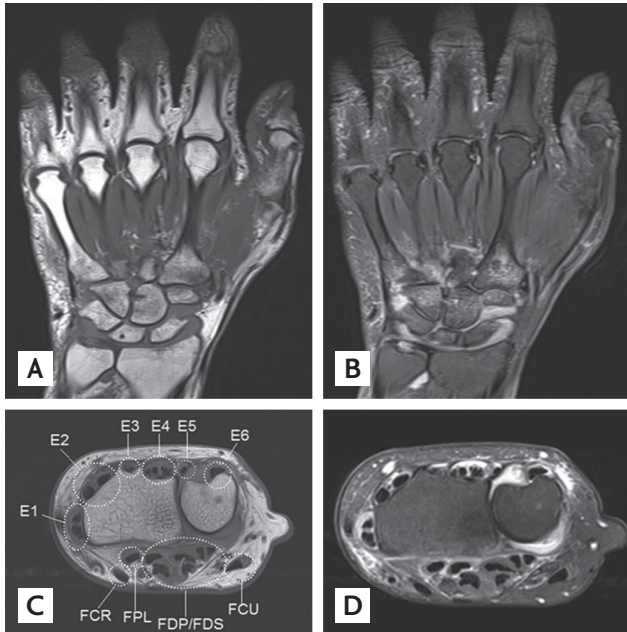


Figure 1. Magnetic resonance imaging (MRI) for detection of bone erosion, bone marrow edema, synovitis, and tenosynovitis. (A) T1-weighted coronal image and (B) corresponding T2-weighted coronal image. The MRI scans show bone marrow edema in the 2nd, 3rd, and 5th metacarpal bases and in the capitate, hamate, and trapezoid. They show bone erosion in the capitate, scaphoid, distal radius, and 5th metacarpal base, with synovitis of the 3rd to 5th carpometacarpal, intercarpal, and radiocarpal joints. (C) T1-weighted axial image and (D) corresponding T2-weighted axial image at wrist level. The 6 extensor compartments at the wrist dorsum are defined under the extensor retinaculum and are covered with a synovial sheath containing the extensor pollicis brevis and abductor pollicis longus (E1), extensor carpi radialis brevis and extensor carpi radialis longus (E2), extensor pollicis longus (E3), extensor digitorum communis and extensor indicis proprius (E4), extensor digiti quinti proprius (E5), and extensor carpi ulnaris (E6). On the palmar side, the flexor tendons in the carpal tunnel are covered by the synovium of the radial and ulnar bursa. The flexor tendons are composed of (1) the flexor carpi ulnaris (FCU); (2) ulnar bursa, including the flexor digitorum profundus and superficialis tendon quartets (FDP/FDS); (3) flexor pollicis longus (FPL) in the radial bursa; and (4) flexor carpi radialis (FCR). The MRI scans show tenosynovitis in all extensor tendons and in the FCR, FPL, and FDP.

is a sharply margined bone lesion with correct juxta-articular localization and typical signal characteristics that is visible on two planes, with observation of a cortical break on at least one plane. The bone erosions were scored on a scale of 0 to 10 based on the proportion of eroded bone to the assessed bone volume as judged from all available images, as follows: 0, no erosion; 1,

1% to 10% of bone eroded; 2, 11% to 20% of bone eroded, etc. MRI-detected BME is a lesion in the trabecular bone with ill-defined margins and signal characteristics consistent with increased water content. The BME scale ranged from 0 to 3 and was used to rate the proportion of bone with edema as follows: 0, no edema; 1, 1% to 33% of edematous bone; 2, 34% to 66% of edematous bone; 3, 67% to 100% of edematous bone. Synovitis presents as an area in the synovial compartment that shows an increased signal on T2-weighted fat-suppressed images and a thickness greater than the width of the normal synovium. It was assessed as being present or absent without being graded in 4 wrist regions—the distal radioulnar joint, the radiocarpal joint, the intercarpal joint, and the CMC joint—and in each MCP joint. The MRI-detected tenosynovitis was evaluated as described by Haavardsholm et al. [10]. In MRI, tenosynovitis is visualized as tendon sheath fluid, sheath thickening, and an increased signal on T2-weighted fat-suppressed images. A total of 10 separate anatomical areas of the wrist were assessed for tenosynovitis: the six extensor compartments and four regions on the volar side, namely, the flexor carpi ulnaris, the ulnar bursa including the flexor digitorum profundus and superficialis (FDP/FDS), the flexor pollicis longus in the radial bursa, and the flexor carpi radialis (FCR) (Fig. 1C and 1D).

Statistical analysis

All statistical analyses were performed with the IBM SPSS version 23.0 (IBM Co., Armonk, NY, USA). The continuous variables were expressed as mean \pm standard deviation, and the categorical variables were presented as frequencies and proportions. The results were compared with Pearson chi-square test, Fisher exact test, a chi-square test for trend, and the Mann Whitney *U* test or Kruskal-Wallis test as appropriate. A logistic regression analysis was used to control the treatment and disease duration variables associated with MRI-detected abnormalities. A *p* value < 0.05 was considered significant.

RESULTS

Clinical characteristics

The baseline characteristics of the patients are present-

ed in Table 1. The distributed patterns of bone erosion, BME, synovitis, and tenosynovitis on the MR images were compared between the patients with SPRA and those with SNRA. The patients with SPRA showed longer disease durations than those with SNRA (26.4 ± 29.0 months vs. 13.7 ± 12.5 months, $p = 0.044$). No difference was observed in the ESR, CRP, and prior treatment of RA of the two groups of patients.

Bone erosion and BME

A total of 78.3% and 69.6% of RA patients presented bone erosion and BME at the wrist, respectively. The carpal bones were more frequently affected by bone erosion and BME than the metacarpal or phalangeal bones that compose the MCP joints. The capitate bone was most frequently affected by erosion, followed by the lunate, the triquetrum, the hamate, and the distal radius. BME was most frequent in the 2nd phalangeal base, followed by the lunate, the capitate, the triquetrum, the hamate, and the trapezoid (Fig. 2A). Carpal bone lesions caused by erosion with BME were most frequent in the capitate, followed by the lunate, the triquetrum, the scaphoid, the trapezoid, and the distal radius (data not shown). A total of 34.2% and 29.0% of RA patients had bone erosion and

BME at the MCP joint, respectively. In the MCP joints, the 2nd phalangeal base was the most commonly affected by bone erosion and BME, followed by the 2nd, 3rd, and 4th metacarpal heads (data not shown). The results were similar in treatment-naïve RA patients ($n = 12$). The capitate bone was the bone most frequently affected by erosion and BME, followed by the lunate and the hamate.

For the bone erosion, the average sum scores of the unilateral wrist joints and second to fifth joints were 10.5 and 2.1, respectively. The corresponding values for the BME were 5.3 and 1.5, respectively. The capitate also had the highest RA-MRI bone erosion score, followed by the lunate, the triquetrum, the hamate, the distal ulna, and the radius, whereas the 2nd phalangeal base had the highest RA-MRI BME score, followed by the lunate, the capitate, the 4th metacarpal base, and the triquetrum (Fig. 2B).

The analysis according to the seropositivity status showed that at least one location scored positive for bone erosion in 68.8% of SPRA patients and in 100% of SNRA patients, while the corresponding values for BME were 68.8% and 74.4%, respectively. After controlling for the disease duration and treatment received, there

Table 1. Baseline characteristics of 43 RA patients involved in magnetic resonance imaging study

Characteristic	Total RA (n = 43)	SPRA (n = 31)	SNRA (n = 12)	p value
Age, yr	53.4 ± 14.4 (28–78)	52.1 ± 14.6 (28–78)	56.8 ± 13.9 (35–75)	0.364 ^a
Sex, male/female (% of female)	8/35 (81.4)	3/28 (90.3)	5/7 (58.3)	0.023 ^b
Disease duration, mon	23.0 ± 26.0 (1–120)	27.0 ± 29.2 (1–120)	14.9 ± 13.2 (1–36)	0.032 ^a
RF or anti-CCP positivity	31 (72.1)	31 (100.0)	0	< 0.001 ^b
RF positivity	27 (62.8)	27 (87.1)	0	< 0.001 ^b
Anti-CCP positivity	30 (69.8)	30 (96.7)	0	< 0.001 ^b
ESR, mm/hr	31.7 ± 27.6 (2–120)	29.8 ± 25.1 (2–81)	36.6 ± 33.9 (7–120)	0.702 ^a
CRP, mg/dL	2.1 ± 5.2 (0.0–27.50)	1.8 ± 5.1 (0.01–27.50)	2.9 ± 5.7 (0.01–20.30)	0.095 ^a
Treatment prior to study, %				
Naïve	23.3	16.1	41.7	0.087 ^b
csDMARDs	69.8	74.2	58.3	0.495 ^b
TNF inhibitor	6.9	9.7	0	0.543 ^b

Values are presented as mean ± SD (range) or number (%).

RA, rheumatoid arthritis; SPRA, seropositive rheumatoid arthritis; SNRA, seronegative rheumatoid arthritis; RF, rheumatoid factor; CCP, cyclic citrullinated peptide; ESR, erythrocyte sedimentation rate; CRP, C-reactive protein; csDMARDs, conventional synthetic disease modifying antirheumatoid drugs; TNF, tumor necrosis factor.

^aSignificant using Mann-Whitney U test.

^bSignificant using chi-square test.

were no differences between the RA-MRI scoring patterns and the bone erosion and BME between SPRA and SNRA patients.

Synovitis

A total of 80.4% of patients presented synovitis at the wrist. The carpal joints were more affected by synovitis than the MCP joints. Synovitis was most frequently detected in the intercarpal joint, followed by the radiocarpal, radioulnar, and CMC joints. Among the MCP joints,

the 2nd MCP joint was the most frequently affected, followed by the 3rd, 4th, and 5th MCP joints. Although this is not included in the OMERACT RAMRIS, RA-associated synovitis was also found in 12.8% of the patients' 1st MCP joints (Fig. 3).

At least one location scored positive for synovitis in 81.4% of SPRA patients and in 92.9% of SNRA patients. After controlling for the disease duration and treatment received, there was no difference in the RA-MRI synovitis scoring patterns of the SPRA and SNRA patients.

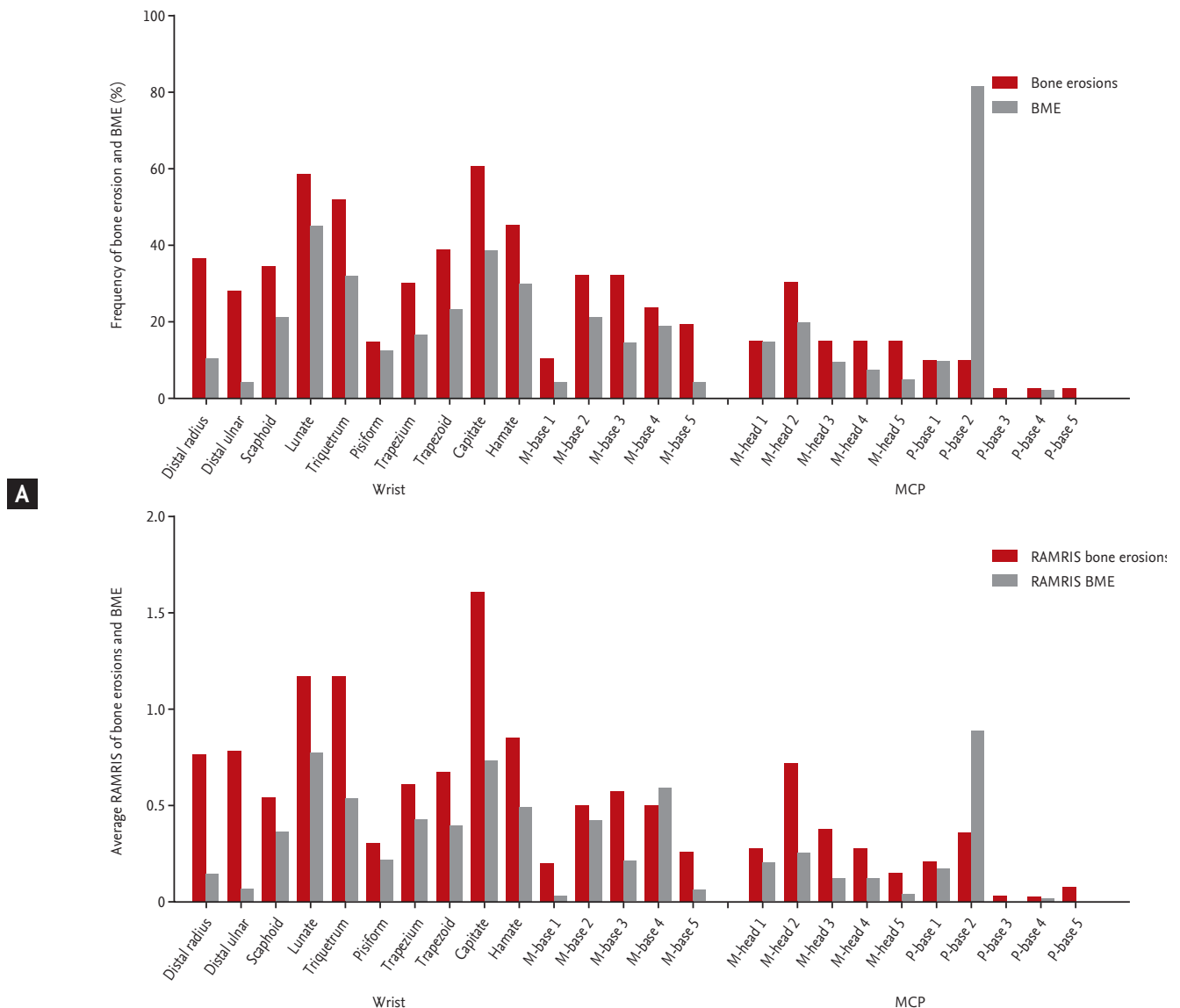


Figure 2. (A) Frequency of bone erosion and bone marrow edema (BME) per bone at the wrist and metacarpophalangeal (MCP) joints in patients with rheumatoid arthritis (RA). (B) Average RA-magnetic resonance imaging score (RAMRIS) for bone erosion and BME per bone at the wrist and MCP joints in patients with RA. M, metacarpal; P, proximal phalangeal.

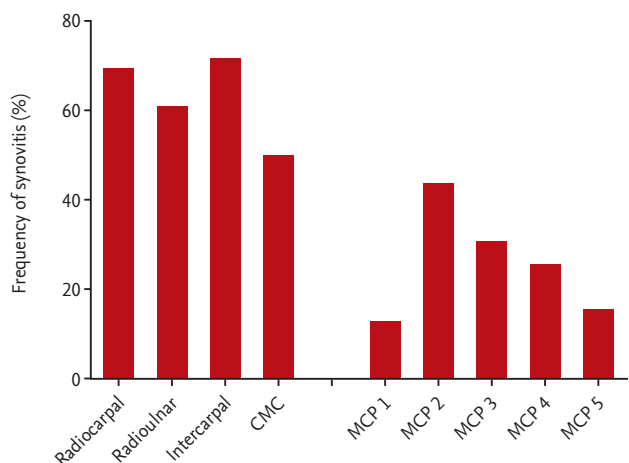


Figure 3. Synovitis frequency at each wrist and metacarpophalangeal (MCP) joint. CMC, carpometacarpal.

Tenosynovitis

A total of 78.3% of patients had tenosynovitis around the wrists; 56.5% had tenosynovitis of the flexor tendons, while 52.2% presented it at the extensor tendons, and 32.6% had both. The FDP/FDS were most frequently affected (43.5%), followed by the tendons of extensor compartments 4, 2, and 6 (Fig. 4A). The results were similar in treatment-naïve RA patients. The FDP/FDS was most frequently affected, followed by the FCR and the tendons of the extensor compartment 2.

Although there was no difference in terms of synovitis, bone erosion, and BME between the SPRA and SNRA patients, those with SNRA had more tenosynovitis than those with SPRA. At least one location scored positive for tenosynovitis in 92.9% of SNRA patients, which represented a higher prevalence than in SPRA patients (71.9%). After controlling for the disease duration and treatment received, SNRA patients also showed significantly more inflammation in both extensor tendons, particularly in the wrist extensor compartments 3 and 4 (78.6%, 35.7%, and 50.0%; $p = 0.04$, $p = 0.04$, and $p = 0.03$, respectively) (Fig. 4B).

DISCUSSION

This study aimed to evaluate the patterns of bone ero-

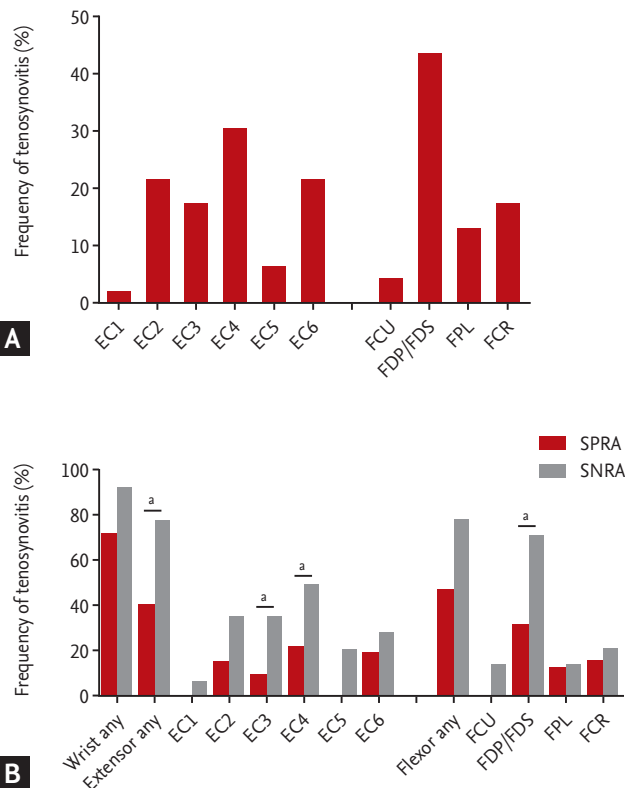


Figure 4. (A) Tenosynovitis frequency at each evaluated location. Extensor compartments (ECs) 1 to 6 mean compartments of extensor tendons in the wrist containing: (1) the extensor pollicis brevis and abductor pollicis longus; (2) extensor carpi radialis brevis and extensor carpi radialis longus; (3) extensor pollicis longus; (4) extensor digitorum communis and extensor indicis proprius; (5) extensor digiti quinti proprius; and (6) extensor carpi ulnaris. The flexor tendon areas in the wrist include: (1) the flexor carpi ulnaris (FCU); (2) ulnar bursa, including the flexor digitorum profundus and superficialis tendon quartets (FDP/FDS); (3) flexor pollicis longus (FPL) in the radial bursa; and (4) flexor carpi radialis (FCR). (B) Tenosynovitis frequency at each evaluated location in wrist joint of all patients with rheumatoid arthritis (RA), of patients with seropositive rheumatoid arthritis (SPRA), and of patients with seronegative rheumatoid arthritis (SNRA). ^a $p < 0.05$ (vs. SPRA).

sion, BME, synovitis, and tenosynovitis in the wrist and MCP joints of RA patients using MRI. The MR images were analyzed and rated based on the OMERACT RAMRIS [7-9]. The RAMRIS is a validated method for the scoring of wrist and MCP joint abnormalities. It has been proven to be moderately reliable, to correlate with the disease activity, and to predict the erosive progression and treatment response [5,19]. Several studies have investigated the extent to which RA joint pathologies

could be reliably assessed with unenhanced MRI images rather than with gadolinium (Gd)-enhanced MRI (as the reference method) in order to reduce the imaging time, invasiveness, and cost. Previous research found that the elimination of Gd contrast administration from the MRI procedure did not change the scores of the bone erosion and bone edema but decreased the reliability of the synovitis and tenosynovitis scores [20,21]. Based on these prior findings, we explored the bone erosion and BME RAMRISs, but only investigated the presence or absence of synovitis and tenosynovitis without scoring them.

The disease duration of RA and presence of RF or anti-citrullinated protein antibody (ACPA) have been known as a prognostic factor of poor functional and radiographic outcomes [22]. However, because of the small sample size and the inhomogeneity, we found no differences in the MRI-detected erosion, BME, and synovitis between SPRA and SNRA patients. Further large-scale studies are needed to reveal the differences in MRI-detected abnormalities according to the seropositivity status.

The patterns of RA involvement in the wrist and MCP joints were identified based on data obtained from 46 MR scans of 43 RA patients. The capitate, lunate, triquetrum, and hamate bones, together with the 2nd MCP joint were most frequently affected by bone erosion and BME. The distribution of the MRI-detected erosion and BME in RA patients in this study was similar to that in previous reports [17,23,24]. Regarding MRI-detected synovitis in the wrist joints, it was most frequently detected in the intercarpal joint, echoing the results of previous reports [23]. The overall results for the most common sites of erosion, BME, and synovitis matched the findings of previous studies. However, our study showed not only the most commonly affected joints, but also the specific prevalence of MRI-detected abnormalities and the RAMRIS.

Moreover, we observed MRI-detected tenosynovitis in 78.3% of RA patients, and found that the extensor compartment 4 and the FDP/FDS were frequently affected. Likewise, Nieuwenhuis et al. [16] showed the prevalence of MRI-detected tenosynovitis in RA patients was 75%, and the extensor compartments 6 and 4 were the most commonly affected sites. Interestingly, the study showed that SNRA patients were significantly more affected by tenosynovitis in the extensor tendons, particularly in the wrist extensor compartments 3 and 4. Although the

synovitis and BME burdens are predictive of future radiologic joint destruction, the prognostic value of tenosynovitis for the latter is unknown [25]. The results of our study were consistent with those of Nieuwenhuis et al. [16], which suggested that there was no association between ACPA positivity and tenosynovitis. Synovitis is a rich source of proinflammatory cytokines, which drive the process of osteoclast differentiation. It can lead to degradation of the cartilage and bone through osteoclastogenesis [26]. Similarly to the synovium, in RA patients, the tenosynovium produces proinflammatory cytokines and proteolytic enzymes. Tenosynovitis can also cause impaired function from scarring and adhesion [22,27]. Theoretically, inflamed tendon sheaths, which pass by the bone surface, can spread inflammation from the tendon to the articular synovium [28]. However, it remains uncertain whether MRI-detected tenosynovitis is a prognostic factor of bone erosion in clinical practice. Further prospective studies are required to determine the prognostic value of tenosynovitis for RA.

It is also crucial to note that the first MCP joint was the second most frequent site of bone erosion and BME in the MCP joints. Arthritis of the first MCP joint is excluded from the OMERACT-RAMRIS, as this joint is commonly affected by osteoarthritis [18,25]. Regarding the hand function of patients with RA, the thumb has been identified as the most consistent indicator of impaired hand function [26]. It might be useful to investigate the potential value of the first MCP joint as an additional MR parameter for further development of the RA-MRI scoring system.

Our study presented several limitations. First, the statistical power was limited by the small sample size of 46 MR scans. To evaluate the association between seropositivity and MRI-detected abnormalities, we aimed to form four subgroups according to the presence or absence of both RF and anti-CCP Ab (RF⁻/anti-CCP Ab⁻, RF⁺/anti-CCP Ab⁻, RF⁻/anti-CCP Ab⁺, and RF⁺/anti-CCP Ab⁺). However, this was prevented by the small sample sizes of the single seropositive patient group (n = 6) and of the double seronegative patient group (n = 11). Second, the retrospective design of this study represented a shortcoming. Certain clinical parameters, such as the disease activity score 28 (DAS 28) and the simplified disease activity index (SDAI) score, could not be evaluated through the retrospective chart reviews. Third, as the

obtained MR images were nonenhanced, a quantitative approach to synovitis and tenosynovitis could not be taken. Fourth, the MR images were non-independently evaluated in consensus by two readers, and we could not present the inter-reader reliability.

The OMERACT RAMRIS is known as the most mature quantitation system for RA [4]. Nevertheless, the complex and time-consuming nature of the procedure makes it difficult to apply in clinical practice. Future studies should consider whether a simplified version of the RAMRIS focusing on the most frequently involved bones and tendons could be developed as a validation process. A modified and simplified RAMRIS based on commonly involved bones and tendons might shorten the time needed for image analysis, thus facilitating the use of MRI in various RA clinical studies.

In conclusion, this study identified the distribution and prevalence of MRI-detected bone erosion, BME, synovitis, and tenosynovitis of the wrist and MCP joints in RA patients. The patterns of the MRI-detected abnormalities may help to select sites for the application of MRI protocols in clinical trials and practice.

KEY MESSAGE

1. The capitate, lunate, triquetrum, and hamate bones were the most common sites of erosion and bone marrow edema (BME), and demonstrated the highest rheumatoid arthritis (RA)-magnetic resonance imaging (MRI) score (RAMRIS) erosion and BME scores.
2. MRI-detected tenosynovitis was present in 78.3% of all patients with RA. The extensor compartment 4 and flexor digitorum profundus/superficialis were frequently affected.

Conflict of interest

No potential conflict of interest relevant to this article was reported.

Acknowledgments

This research was supported by the Basic Science Research Program, through the National Research Foundation of Korea (NRF), and funded by the Ministry of Education, Science and Technology (2015R1D1A1A01056763).

REFERENCES

1. Grassi W, De Angelis R, Lamanna G, Cervini C. The clinical features of rheumatoid arthritis. *Eur J Radiol* 1998;27 Suppl 1:S18-S24.
2. Klareskog L, Catrina AI, Paget S. Rheumatoid arthritis. *Lancet* 2009;373:659-672.
3. Scott DL, Bacon PA. Joint damage in rheumatoid arthritis: radiological assessments and the effects of anti-rheumatic drugs. *Rheumatol Int* 1985;5:193-199.
4. Hodgson RJ, O'Connor P, Moots R. MRI of rheumatoid arthritis image quantitation for the assessment of disease activity, progression and response to therapy. *Rheumatology (Oxford)* 2008;47:13-21.
5. Mathew AJ, Danda D, Conaghan PG. MRI and ultrasound in rheumatoid arthritis. *Curr Opin Rheumatol* 2016;28:323-329.
6. Sewerin P, Buchbender C, Vordenbaumen S, et al. Advantages of a combined rheumatoid arthritis magnetic resonance imaging score (RAMRIS) for hand and feet: does the RAMRIS of the hand alone underestimate disease activity and progression? *BMC Musculoskelet Disord* 2014;15:104.
7. Ejbjerg B, McQueen F, Lassere M, et al. The EULAR-OMERACT rheumatoid arthritis MRI reference image atlas: the wrist joint. *Ann Rheum Dis* 2005;64 Suppl 1:i23-i47.
8. Ostergaard M, Edmonds J, McQueen F, et al. An introduction to the EULAR-OMERACT rheumatoid arthritis MRI reference image atlas. *Ann Rheum Dis* 2005;64 Suppl 1:i3-i7.
9. Conaghan P, Bird P, Ejbjerg B, et al. The EULAR-OMERACT rheumatoid arthritis MRI reference image atlas: the metacarpophalangeal joints. *Ann Rheum Dis* 2005;64 Suppl 1:i11-i21.
10. Haavardsholm EA, Ostergaard M, Ejbjerg BJ, Kvan NP, Kvien TK. Introduction of a novel magnetic resonance imaging tenosynovitis score for rheumatoid arthritis: reliability in a multireader longitudinal study. *Ann Rheum Dis* 2007;66:1216-1220.
11. Ostergaard M, Peterfy C, Conaghan P, et al. OMERACT Rheumatoid Arthritis Magnetic Resonance Imaging Studies: core set of MRI acquisitions, joint pathology definitions, and the OMERACT RA-MRI scoring system. *J Rheumatol* 2003;30:1385-1386.
12. Haavardsholm EA, Ostergaard M, Ejbjerg BJ, et al. Reli-

- ability and sensitivity to change of the OMERACT rheumatoid arthritis magnetic resonance imaging score in a multireader, longitudinal setting. *Arthritis Rheum* 2005; 52:3860-3867.
13. Ostergaard M, Emery P, Conaghan PG, et al. Significant improvement in synovitis, osteitis, and bone erosion following golimumab and methotrexate combination therapy as compared with methotrexate alone: a magnetic resonance imaging study of 318 methotrexate-naive rheumatoid arthritis patients. *Arthritis Rheum* 2011;63:3712-3722.
 14. Cohen SB, Dore RK, Lane NE, et al. Denosumab treatment effects on structural damage, bone mineral density, and bone turnover in rheumatoid arthritis: a twelve-month, multicenter, randomized, double-blind, placebo-controlled, phase II clinical trial. *Arthritis Rheum* 2008; 58:1299-1309.
 15. Ranganath VK, Motamedi K, Haavardsholm EA, et al. Comprehensive appraisal of magnetic resonance imaging findings in sustained rheumatoid arthritis remission: a substudy. *Arthritis Care Res (Hoboken)* 2015;67:929-939.
 16. Nieuwenhuis WP, Krabben A, Stomp W, et al. Evaluation of magnetic resonance imaging-detected tenosynovitis in the hand and wrist in early arthritis. *Arthritis Rheumatol* 2015;67:869-876.
 17. Ostergaard M, Moller Dohn U, Duer-Jensen A, et al. Patterns of magnetic resonance imaging bone erosion in rheumatoid arthritis: which bones are most frequently involved and show the most change? *J Rheumatol* 2011;38: 2014-2017.
 18. Aletaha D, Neogi T, Silman AJ, et al. 2010 Rheumatoid arthritis classification criteria: an American College of Rheumatology/European League Against Rheumatism collaborative initiative. *Arthritis Rheum* 2010;62:2569-2581.
 19. Baker JF, Tan YK, Conaghan PG. Monitoring in established RA: role of imaging and soluble biomarkers. *Best Pract Res Clin Rheumatol* 2015;29:566-579.
 20. Stomp W, Krabben A, van der Heijde D, et al. Aiming for a simpler early arthritis MRI protocol: can Gd contrast administration be eliminated? *Eur Radiol* 2015;25:1520-1527.
 21. Ostergaard M, Conaghan PG, O'Connor P, et al. Reducing invasiveness, duration, and cost of magnetic resonance imaging in rheumatoid arthritis by omitting intravenous contrast injection: does it change the assessment of inflammatory and destructive joint changes by the OMERACT RAMRIS? *J Rheumatol* 2009;36:1806-1810.
 22. de Vries-Bouwstra JK, Goekoop-Ruiterman YP, Verpoort KN, et al. Progression of joint damage in early rheumatoid arthritis: association with HLA-DRB1, rheumatoid factor, and anti-citrullinated protein antibodies in relation to different treatment strategies. *Arthritis Rheum* 2008; 58:1293-1298.
 23. Olech E, Crues JV 3rd, Yocum DE, Merrill JT. Bone marrow edema is the most specific finding for rheumatoid arthritis (RA) on noncontrast magnetic resonance imaging of the hands and wrists: a comparison of patients with RA and healthy controls. *J Rheumatol* 2010;37:265-274.
 24. Tani C, D'Aniello D, Possemato N, et al. MRI pattern of arthritis in systemic lupus erythematosus: a comparative study with rheumatoid arthritis and healthy subjects. *Skeletal Radiol* 2015;44:261-266.
 25. Berger AJ, Meals RA. Management of osteoarthritis of the thumb joints. *J Hand Surg Am* 2015;40:843-850.
 26. Vliet Vlieland TP, van der Wijk TP, Jolie IM, Zwinderman AH, Hazes JM. Determinants of hand function in patients with rheumatoid arthritis. *J Rheumatol* 1996;23:835-840.
 27. Jain A, Nanchahal J, Troeberg L, Green P, Brennan F. Production of cytokines, vascular endothelial growth factor, matrix metalloproteinases, and tissue inhibitor of metalloproteinases 1 by tenosynovium demonstrates its potential for tendon destruction in rheumatoid arthritis. *Arthritis Rheum* 2001;44:1754-1760.
 28. Hayer S, Redlich K, Korb A, Hermann S, Smolen J, Schett G. Tenosynovitis and osteoclast formation as the initial preclinical changes in a murine model of inflammatory arthritis. *Arthritis Rheum* 2007;56:79-88.